

Cooperative Recognition of Ni²⁺ Triggered by Fluoride Ions in Naturally Occurring α -Hydroxyquinone Derivatives

Mario Valle-Sánchez, Claudia A. Contreras-Celedón, Adrián Ochoa-Terán, and Luis Chacón-García*

Cite This: *ACS Omega* 2021, 6, 16419–16427

Read Online

ACCESS |



Metrics & More

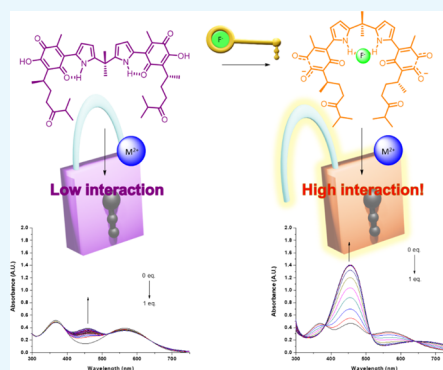


Article Recommendations



Supporting Information

ABSTRACT: Perezone is a naturally occurring hydroxyquinone that has been deeply studied from different chemical aspects, such as therapeutics, electrochemistry, physical–chemical properties, or synthetic approaches that turn it an attractive template for new semisynthetic derivatives with a wide range of purposes. Herein, we describe a facile synthetic pathway to obtain new perezone derivatives by the addition of a pyrrole moiety that can be used for ion recognition. Compounds 2–4 showed the capability to interact with several anions and M²⁺ cations as separate events that result in colorimetric changes. Moreover, the compounds can behave as heteroditopic receptors. Besides, a previous interaction between fluoride ions and perezone derivatives triggered a successful recognition of M²⁺ ions, remarking Ni²⁺ as the most interesting phenomenon. These results project the compounds as potential colorimetric receptors for nickel ions in complex solutions.



INTRODUCTION

Chemical entities with supramolecular activity, such as molecular receptors, provide the building blocks for biological markers, molecular machines and smart polymers, among others. Recognition of chemical species is a fast-developing area in supramolecular chemistry due to its implications in pollution, materials, foods, drugs, and animal physiology.^{1–4} In this sense, molecular recognition of biologically important anions is currently an expanding area in the field of supramolecular chemistry that has the continuous urgency for developing anion sensors for complex media such as blood, serum, drinking water, and other biological systems.^{5–7}

Certain metallic species are in the spotlight of biological, chemical, and interdisciplinary studies by playing a pivotal role in many intra- and extracellular functions. However, these can only be monitored *in vitro* by using potentiometric single-ion selective sensors.

Even though most of the chemical sensing for cation recognition is focused on determining the biological activities of ions such as calcium (Ca), magnesium (Mg), iron (Fe), or copper (Cu), nocive effects of some metal cations remain in the shadow due to their apparent innocuousness, that is, in the cases of cobalt (Co), nickel (Ni), and chromium (Cr) that are used in prosthesis manufacturing because of their high mechanical stability and good biological compatibility, their corrosion products have been shown to provoke adverse biological responses. Highlighting nickel and nickel derivatives, it is also known that chronic exposure to these compounds can cause allergies, inflammatory processes, and prevalence of lung carcinoma; the general population consumes most of the nickel through food; the average daily intake of nickel from food in

the United States is estimated to be 150–168 μg . A typical daily intake from drinking water is about 2 μg and from air is 0.1–1 μg . The general population is also exposed to nickel in nickel alloys and nickel-plated materials, such as coins, steel, and jewelry, and residual nickel may be found in soaps, fats, and oils.^{8–10}

Although sensing cationic ions has received more attention in supramolecular chemistry, recognition of anionic species has been emerging in the last 3 decades.¹¹

Anions are essential to maintain the adequate functions of both biological and industrial processes and are often found as harmful pollutants.¹² For instance, perchlorate ions are highly water-soluble environmental contaminants, so they can readily move to aqueous media, resulting in the contamination of groundwater and could also disrupt normal thyroid functions competing with iodide.¹³ It is also well known that chronic exposure to aqueous fluoride in concentrations above 1 ppm causes various diseases in organisms, such as dental and skeletal fluorosis, increased susceptibility to kidney disease, and cancer, as well as involvement in a delay of neurological development and reduced IQ in school-age children.^{14,15} Elusive anions such as fluoride can be recognized and captured by hydrogen bonding with protonated nitrogen groups.¹⁶ A class of ion receptors that always attract a great deal of interest

Received: March 16, 2021

Accepted: June 8, 2021

Published: June 17, 2021



are those that simultaneously coordinate both anionic and cationic guest species. A consequence of binding both cations and anions in the same receptor is a decrease in the energy cost of the recognition process.¹⁷ Like anion- and cation-sensing, ion-pair recognition also has multiple applications as sensors, membrane transport, salt solubilization, or extraction agents, to name a few.^{11,18,19}

Recent reports in the area of anion recognition describe a wide variety of neutral, relatively simple-to-synthesize, and acyclic anion receptors based on pyrrole, indole, or amide groups and their combinations with remarkable anion-binding properties.²⁰ Pyrrole can recognize anions due to its nature of donating the $-NH$ hydrogen to electron pair receptors. The synthetic versatility of this heterocycle, as well as its ion recognition capability, makes it attractive to be used in supramolecular chemistry, where typical examples are calixpyrroles and porphyrins.²¹ As a counterpart of anion recognizers, cation receptors have oxygen or nitrogen atoms with electron pairs available to be accepted by empty metal orbitals. The most well-known class of cation receptors includes the crown ethers, such as cryptands, podands, calixarenes, and hybrid species.^{22,23}

Cation receptors containing non-ether groups, such as amides or carbonyl fragments, can also act as excellent cation guest recognizers.^{24,25} In particular, quinones have two carbonyl groups that could recognize cations via Lewis acid–base interactions; however, they have been poorly studied for such purposes, although they are of great interest in synthetic processes and biological systems. Anion–quinone interactions have been studied theoretically.²⁶

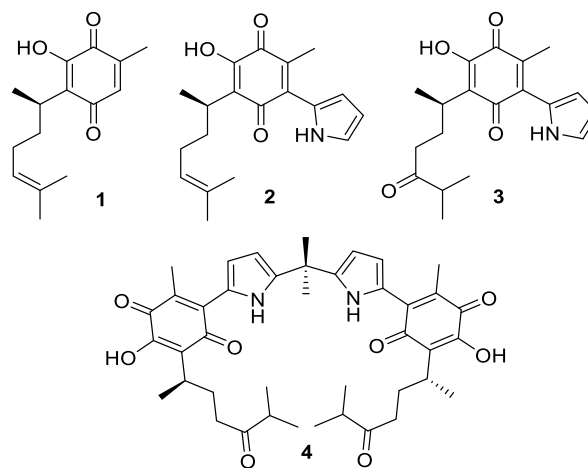
Some quinones have been examined as cation or anion receptors,^{27–29} for example, benzoquinone has been reported to recognize an ion pair;³⁰ the complex of calix-[4]-pyrrole and tetrachloroquinone interact by charge transfer, and the complex can recognize anions.^{31,32}

A new anion receptor, dipyrrolyl quinone,³³ which shows high fluoride specificity, has been described. This receptor presumably recognizes fluoride, both by an anion– π interaction with quinone and by hydrogen bonding with pyrrole. Modifications to pyrrolyl quinones, as well as to quinones, alter their electrochemical properties; the latter phenomenon was recently used for oxidative amidation of aromatic aldehydes.³⁴

It is well known that the building of chemical entities is inspired by such elegant examples taken from natural sources and, in some cases, naturally occurring compounds are the nucleus of the new compounds, considering them as a template with multiple functions that allows the increment of the structure's complexity and sharpens the specificity of the new receptor. Perezone 1 is a naturally occurring *p*-benzoquinone that shows antifeedant and phytotoxic activities,³⁵ inhibition of ADP-induced platelet aggregation,³⁶ promotion of the release of intramitochondrial Ca^{2+} ,³⁷ and remarkable induction of cytotoxicity through the caspase-dependent or caspase-independent mechanism.³⁸ Based on the premises that electron-withdrawing groups bound to pyrrolic compounds tend to increase the compound's binding affinity toward anions, such as fluoride,³⁹ and that quinones interact with ions, we have recently described the synthesis of (*R*)-2-hydroxy-6-methyl-3-(6-methyl-5-oxoheptan-2-yl)-5-(1*H*-pyrrol-2-yl)-cyclohexa-2,5-diene-1,4-dione 3, from perezone 1, designed as an ion-pair receptor.⁴⁰ The behavior of 3 with inorganic salts motivated us to extend the study of compound 4, which in

principle must increase the number of binding sites to evaluate it as a receptor of anions and cations. In this study, we report the heteroditopic receptor abilities of compounds 2–4 toward fluoride and nickel ions (Scheme 1).

Scheme 1. Naturally Occurring Hydroxyquinone Perezone 1 and Its Semisynthetic Derivatives 2–4



RESULTS AND DISCUSSION

Compound 2 was synthesized by the addition of pyrrole to perezone 1 using SiO_2 as the acid promoter of the reaction, as reported previously for compound 3;⁴⁰ the latter compound was used as a control for ion sensing. Dipyrromethane derivative 4 was obtained as a blue-violet amorphous solid by using a green approach to the condensation of (1*H*-pyrrol-2-yl)-4-oxo-perezone 3, with acetone catalyzed by dilute HCl (Scheme 2).⁴¹ Although the condensation of pyrrole with carbonyl compounds has been carried out with trifluoroacetic acid⁴² or $Bi(NO_3)_3 \cdot 5H_2O$ ⁴³ to obtain dipyrromethanes or calix-[4]-pyrroles, in this case, the reaction proceeded with poor yields. The change of the catalyst for dilute HCl in aqueous media considerably increased the yield of the reaction. All compounds were characterized by different available analytical techniques, confirming their structures (Figures S1–S8). The supramolecular behavior of compounds 1–4 was analyzed to discriminate the effect of the side substituents of the hydroxyquinone–pyrrole adduct and the plausible synergism provided by dipyrromethane condensation.

Perezone 1 is an orange solid that has one broad transition band at $\lambda_{max} = 408$ nm, in accordance with previous reports on the starting material; this very broad, low-energy band at $\lambda = 390–415$ nm provides information about the molecule's delocalization system and gives perezone its characteristic color; it may be the product of $n-\pi^*$ transition of the quinone carbonyl groups.⁴⁴ Modifications to 1 at the quinonic moiety can be observed by the naked eye, as the pyrrolyl perezone derivatives 2–4 were all purple. The first comparison of compounds 1 and 2 is shown in Figure 1, where the UV/vis spectra are overlapped. As a first comparison, we can observe just one broad transition band at $\lambda_{max} = 408$ nm for the starting material 1 and a new absorption spectrum that shows a hypsochromic shift (from $\lambda_{max} = 408$ nm to $\lambda_{max} = 360$ nm) and a broad shoulder band that emerges at $\lambda_{max} = 562$ nm; the latter transition has been referred to as the ICT absorption

Scheme 2. Synthetic Pathway Followed to Obtain Compounds 2–4 from Perezone 1

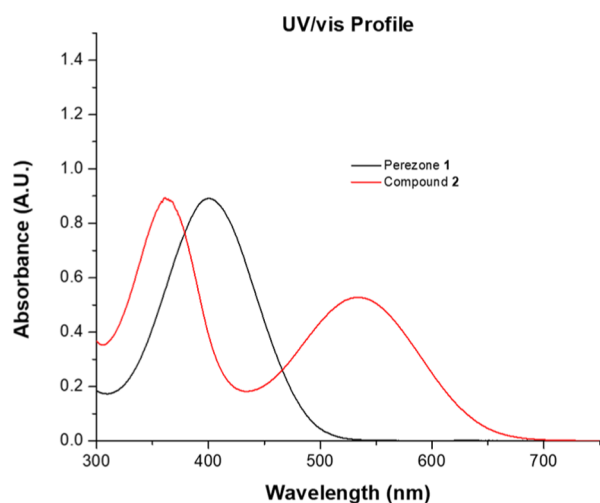
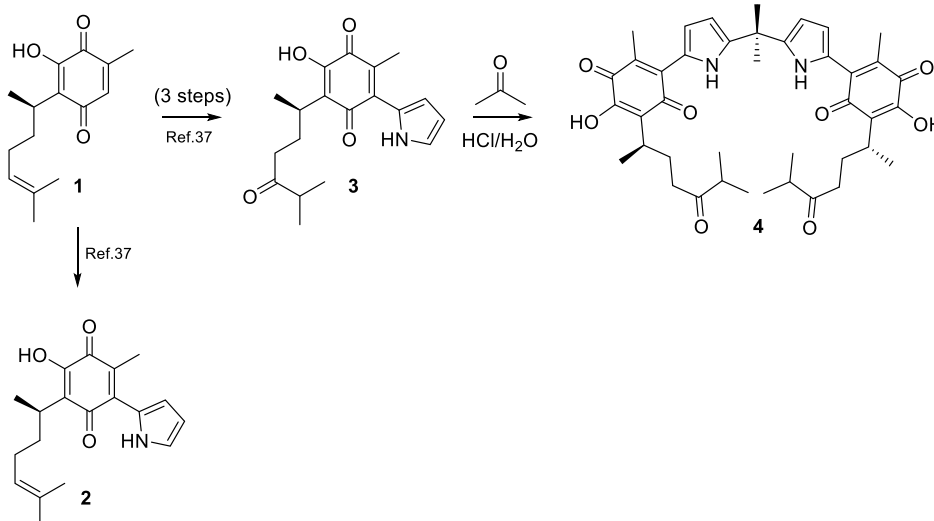


Figure 1. UV/vis spectra for the behavior comparison of perezone 1 and pyrrolyl perezone 2 solutions (1×10^{-5} M in MeCN).

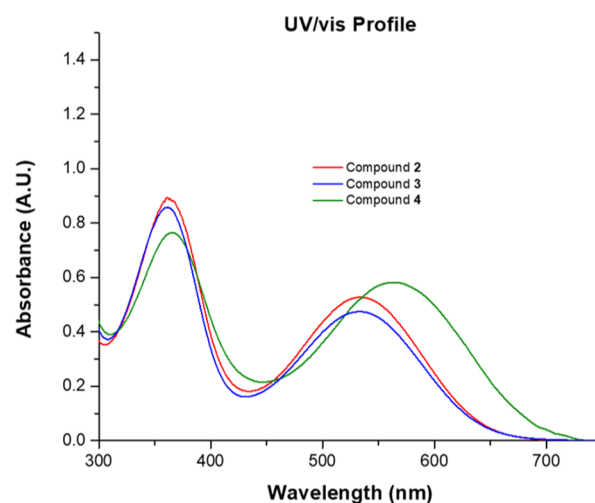


Figure 2. UV/vis spectra of perezone derivatives 2, 3, and 4 solutions (1×10^{-5} M in MeCN).

band mediated by an intermolecular hydrogen bond with the pyrrole moiety.

Perezone derivatives 2 and 4 have been designed to recognize ion pairs and act as colorimetric sensors, as it was reported previously for compound 3, where color changes can be observed for several ion pairs,⁴⁰ before using these compounds toward charged species, we compared the differences at their UV/vis absorption spectra, observing no other significant changes than a slight increase in absorbance and a bathochromic shift for the ICT transition band suffered by compound 4, as shown in Figure 2.

Compounds 2–4 were studied with a series of perchlorate salts including Li^+ , Cd^{2+} , Ni^{2+} , Hg^{2+} , Pb^{2+} , and Zn^{2+} . No significant change was observed using Li^+ and Hg^{2+} , but the formation of a transition band at $\lambda_{\text{max}} = 459$ nm is observed, which correlated with cation–host interaction (Figure S9). This effect (increment of absorbance at $\lambda_{\text{max}} = 459$ nm) follows the order $\text{Ni}^{2+} > \text{Zn}^{2+} > \text{Pb}^{2+} > \text{Cd}^{2+}$, as clearly shown by compound 3 evaluation that was taken as a model in Figure 3.

On the other hand, the compounds were tested as anion receptors, and after the addition of anions to a solution of each derivative, a change in the color from purple ($\lambda_{\text{max}} = 562$ nm)

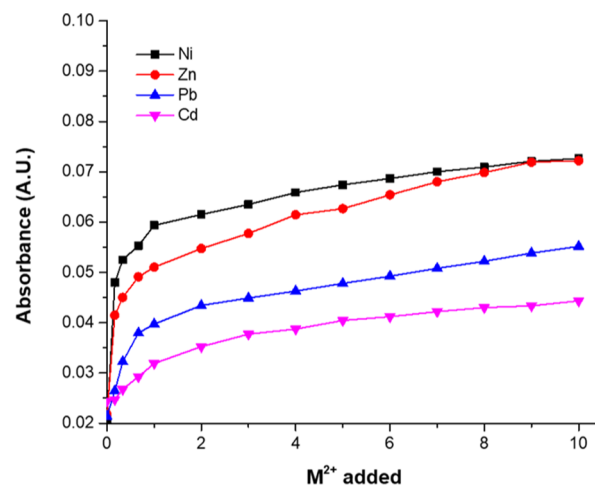


Figure 3. UV/vis spectra for behavior comparison of perezone derivative 3 toward metallic ions.

to yellow ($\lambda_{\text{max}} = 408$ nm) was observed with the more basic anions (Figures S10 and S11); such transition is the same as

that for the starting material, which can be explained by the loss of conjugation with the pyrrole ring which then interacts with the anions, and this behavior is observed in three compounds. Compounds **2** and **3** showed a preference in the order of $\text{CN}^- > \text{F}^- > \text{OH}^- > \text{CH}_3\text{COO}^- > \text{N}_3^-$ (Figures S10 and S11), but compound **4** showed a different pattern as follows: $\text{F}^- > \text{CN}^- > \text{CH}_3\text{COO}^- > \text{N}_3^-$, as depicted in Figure 4. Job's plots for compounds **2–4** with fluoride showed a 1:1 stoichiometry (Figures S13–S15).

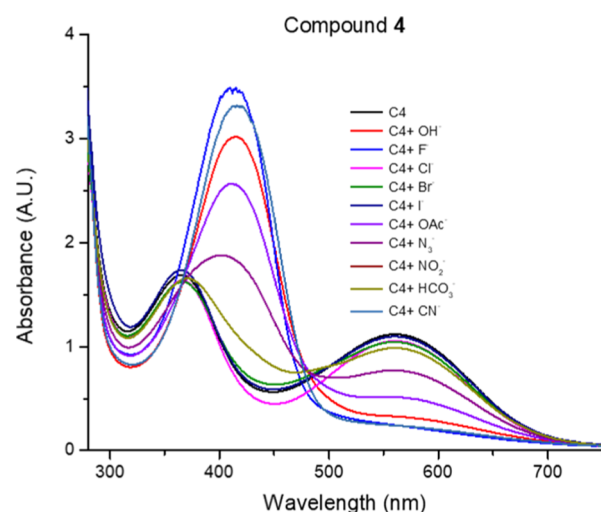


Figure 4. UV/vis spectra for behavior comparison of perezone derivative **4** toward anionic species.

As mentioned above, receptors **3** and **4** were designed to stabilize interactions with the aliphatic carbonyl moiety, so it resulted in the necessity to demonstrate the role of this functional group. In this way, perezone **1** and pyrrolyl perezone derivatives **2** and **3** were evaluated with Ni^{2+} and F^- . For compound **1**, it is known that α -hydroxyquinones act as weak acids, the $\text{p}K_a$ value of which was calculated as <6 , showing $-\text{OH}$ deprotonation in alkaline solutions^{45–47} which translated into a strong bathochromic shift (from $\lambda_{\text{max}} = 400$ to 550 nm). The oxyanionic form is derived from internal proton donors such as the ($-\text{OH}$) group at the C2 position, which, in the presence of strong bases, give a purple color, with the intensity being directly proportional to the amount of perezone.⁴⁴ No appreciable interaction is observed in the UV/vis spectra when a solution of nickel perchlorate was added. It is noteworthy that the bathochromic effect has been appreciated by other authors with topaquinone (a 6-substituted 2-hydroxy-1,4-*p*-benzoquinone) when it was reacted in the presence of a base, indicating a change in the conjugation attributed to the oxyanionic form.⁴⁶ The deprotonation trend is followed by **1**, while tetrabutylammonium fluoride (TBAF) is added even in a Ni^{2+} -saturated solution, where a decrease in absorbance can be observed, probably due to NiF_2 formation. As topaquinone, compound **1** must interact with the metallic ion by coordinating with the hydroxycarbonyl region but with low efficacy at this stage (Figure 5a).

Perezone **1** did not give any interaction with Ni^{2+} , but in the presence of fluoride, the absorption at $\lambda_{\text{max}} = 408$ nm with a shoulder at $\lambda_{\text{max}} = 562$ nm is relevant due to the oxyanion generated by the basicity of the medium already reported for perezone or topaquinone (Figure 5a). The behavior of compounds **2** and **3** is similar but different in comparison

with **1**; both suffered a blue-shifted absorption from $\lambda_{\text{max}} = 530$ nm to 385 nm in the presence of fluoride, instead of the bathochromic effect showed by **1**, which can be attributed to the $\text{NH}\cdots\text{F}$ interaction and the consequent loss of conjugation. This effect has been tracked previously in anion sensing studies (Figures S10 and S11), but the main difference comes from cation sensing, where **2** and **3** show a slightly better interaction with Ni^{2+} than **1**. This interaction increases in the presence of fluoride for both compounds (Figure 5b,c), inferring compounds **2** and **3** are heteroditopic-ion recognizers in comparison with **1**, where the interaction with cations depends on basicity. These results indicated that the contribution of pyrrole is relevant for recognizing the fluoride and the metal ion in the second stage and that the carbonyl in the side chain is helpful, but not expendable, to cause the interaction, as demonstrated by compound **2** where a broad shoulder can be observed at $\lambda_{\text{max}} = 530$ nm. Under these conditions, from ^1H NMR titration (compound **3**, Figure S18), we did not appreciate pyrrole deprotonation. It is important to mention that, as has been discussed in recent works,⁴⁸ the deprotonation of pyrrole by the fluoride anion can be ruled out, considering that its $\text{p}K_a$ value is approximately 16; nevertheless, it is capable of doing so with hydroxyquinone which, as mentioned above, has a $\text{p}K_a$ value of approximately 6, that is considerably more acidic than the heterocycle; so, if such deprotonation would exist, then the equilibrium would shift toward the formation of the oxyanion.

Focusing on compound **4**, after the addition of TBAF to a solution of such derivative, a change in the color from purple ($\lambda_{\text{max}} = 562$ nm) to yellow ($\lambda_{\text{max}} = 408$ nm) was observed, which can be explained by the loss of conjugation between quinone and the pyrrole ring, which then interacts with fluoride in a different way than during only deprotonation (Figure 6a). As shown by the absorbance profile, the stoichiometric ratio for the complex **4**– F^- is 1:1 (Figure S14). $K_f = 1.6 \times 10^5 \text{ M}^{-1}$ was calculated by the adjusted nonlinear minimum square model (Figure S16). On the other hand, the addition of Ni^{2+} to **4** showed a smooth absorption band at $\lambda_{\text{max}} = 459$ nm (Figure 6b), indicating a change in the conjugation of the hydroxyquinone moiety; this is due to the competition with a strong intramolecular hydrogen bond. More interestingly, when Ni^{2+} is added to the TBAF saturated solution of compound **4**, it is observed that the effect on the absorbance at $\lambda_{\text{max}} = 459$ nm (Figure 6c) is still more remarkable than when TBAF is added to the Ni^{2+} saturated solution (Figure 6d), where the band at $\lambda_{\text{max}} = 459$ nm becomes predominant, inferring a cooperative effect on the ditopic recognition. Job's plot of this last interaction shows a 2:1 stoichiometry (Figure S17).

To confirm the interaction of pyrrole with the fluoride anion, ^1H NMR titration was performed for compounds **3** and **4** in anhydrous deuterated acetonitrile with TBAF salt (Figures S18–S20). The ^1H NMR spectra showed that the $-\text{NH}$ “free” proton of pyrrole suffered a downfield shift up to 10.5 ppm, that is, 3–4 ppm downfield from a typical dipyrromethane^{49,50} *prima facie* due to a hydrogen bonding involving quinone's vicinal carbonyl; so, it is expected that fluoride must compete with this intramolecular interaction. A downfield shift of the $-\text{NH}$ signal over 2 ppm was observed up to the saturation of the salt in the mixture (Figures 7 and S19 and S20).

Our proposal of interaction between compound **4** and the tested ions has a “kick-off” as soon as fluoride is added to the solution, generating oxyanionic species, which was observed via

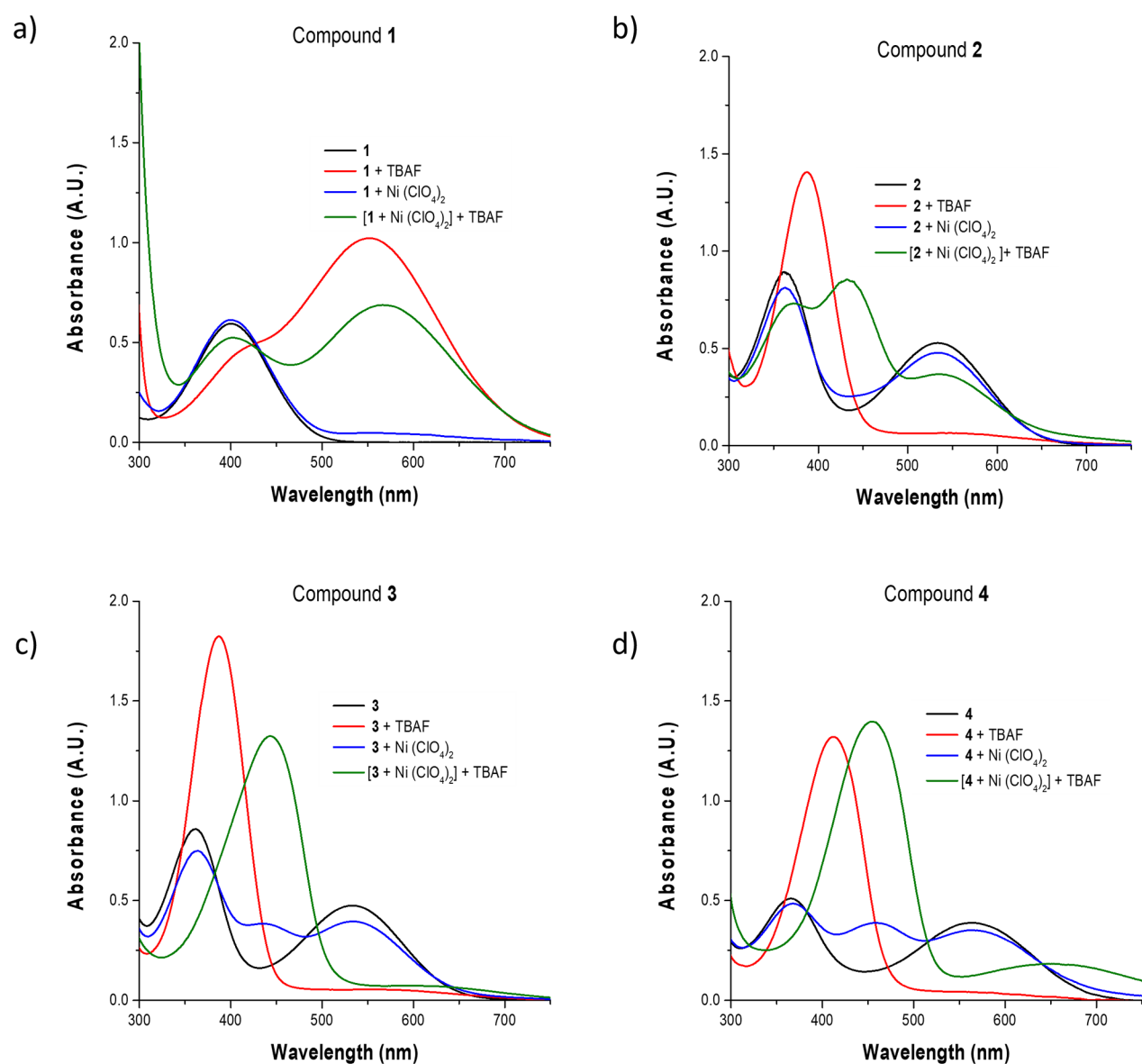


Figure 5. UV/vis spectra for behavior comparison of (a) perezone 1, (b) pyrrolyl perezone 2, (c) pyrrolyl oxoperezone 3, and (d) compound 4.

UV/vis and NMR spectroscopy methods. As the presence of fluoride increases, the interaction leads to a 1:1 complex formed by the dipyrromethane moiety; at this step, we can find the most intense colorimetric shift (hypsochromic, from $\lambda_{\max} = 562$ nm to $\lambda_{\max} = 408$ nm, which was monitored by UV/vis spectroscopy) suffered by 4. The species of the complex $[4 + F^-]$ in the solution can recognize the M^{2+} ions, which can be observed as the new transition band that emerges during both crossed titrations (Scheme 3). This last phenomenon was also reported by Gupta and Mir to generate coordination complexes of hydroxynaphthoquinones and metal ions.^{51,52} The proposed stoichiometry of the last interaction stage is supported by Job's plot, showing a 2:1 ratio of Ni^{2+} ions per $[4 + F^-]$ complex.

A practical advantage of receptor 4 was evaluated toward a solution of commercial toothpaste where a change in coloration from purple to yellow was appreciated at a time when the paste and compound 4 were mixed without a solvent. Moreover, the titration of fluoride was then carried out with a solution of the commercial toothpaste corresponding to 1 mg

F^-/L . 20 μL (0.007 mg F^-) of compound 4 (5×10^{-4} M in CH_3CN) was added to reach 200 μL (0.0625 mg F^-/L). As shown in Figure 8, 4 changes in the absorbance from 0.01 mg/L of the fluoride solution, demonstrating the potential use of this compound as a low-concentration fluoride sensor. This last topic is currently under examination.

CONCLUSIONS

Naturally occurring compounds have potential for application in the construction of complex molecules due to their unique properties and potential ability to generate stimuli-responsive materials and chemical receptors through the use of semi-synthetic approaches. In this work, it was possible to modify specific properties of a naturally occurring chemical entities to create a "multitasking" molecule focused on metal recognition. Compounds 2–4 were synthesized from the naturally occurring compound perezone by clean, economical, and environmentally safe methods; as a case in point, all of these are part of the goals of modern synthetic organic chemistry.⁵³ Although ion sensing is an emerging and fast-evolving area,

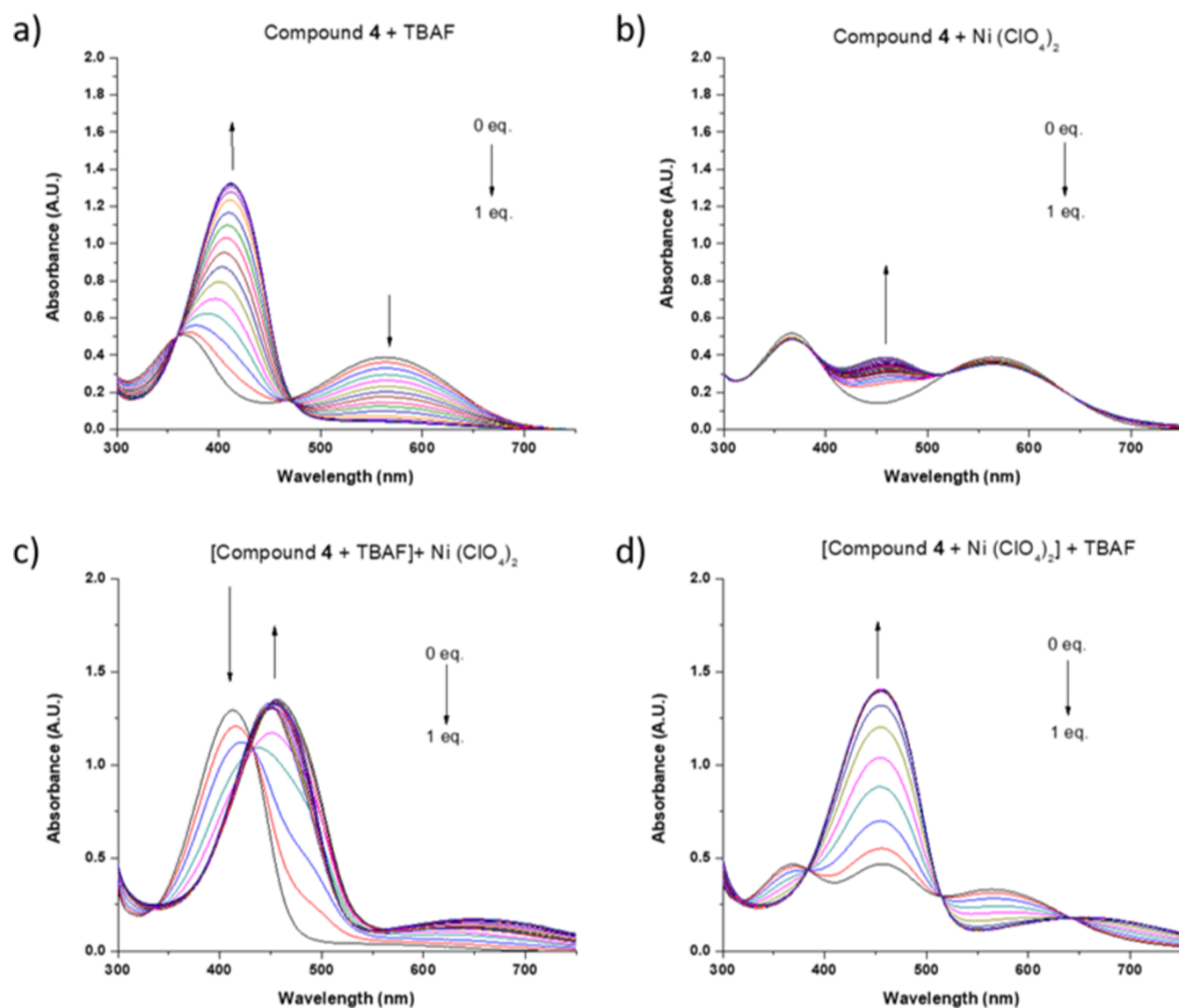


Figure 6. UV/vis spectroscopic titration curves of (a) 4 + TBAF. (b) 4 + Ni(ClO₄)₂. (c) [4 + TBAF] + Ni(ClO₄)₂. (d) [4 + Ni(ClO₄)₂] + TBAF.

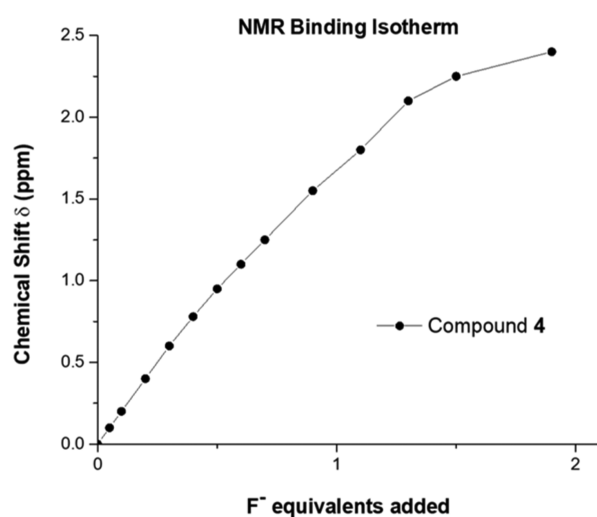


Figure 7. Graphics of the chemical shift observed during the ¹H NMR titration of compound 4 with TBAF in CD₃CN at 22 °C.

only a few reports of ion pair receptor agents from pyrrole–quinone entities have been described.^{30,33,40,54,55} The advantage of functionalizing hydroxyquinones with pyrrole or pyrrole derivatives, such as *meso*-alkyldipyromethanes, involves a synergistic effect; while pyrrole or dipyromethane moieties interact with the anionic species, hydroxyquinone stabilizes the counterion, affording high sensitivity for this unique ion pair (Ni²⁺ and F⁻), even in aqueous solutions and at low concentrations.

EXPERIMENTAL SECTION

General Methods. Nuclear magnetic resonance spectra were recorded on a Varian Mercury 400 spectrometer. ¹H NMR spectra were recorded at 400 MHz and are reported as follows: the chemical shift in ppm is relative to tetramethylsilane (TMS) as an internal standard (for spectra obtained in CDCl₃); multiplicity: s = singlet, d = doublet, t = triplet, q = quartet, m = multiplet, or overlap of nonequivalent resonances. ¹³C NMR spectra were recorded at 100 MHz, and the chemical shift in ppm is relative to TMS from the solvent signal (CDCl₃

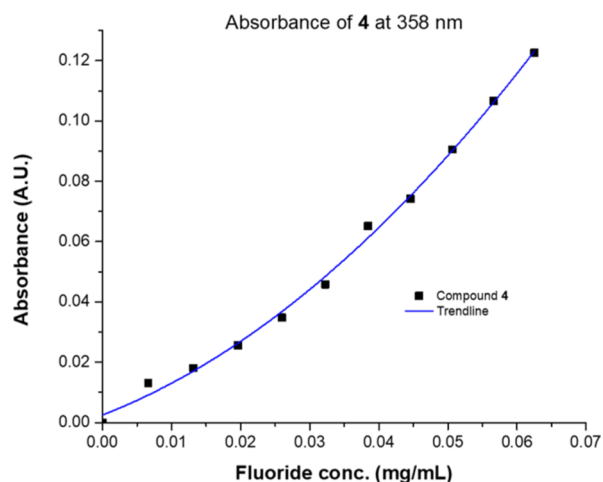
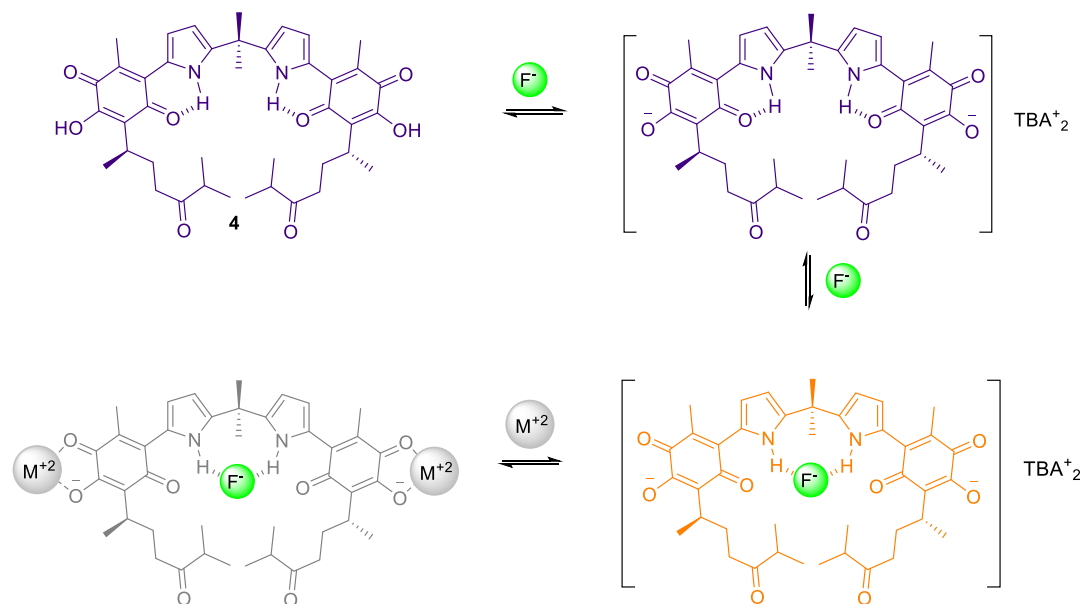
Scheme 3. Interaction Proposal between 4, F⁻, and M²⁺ Species Based on NMR and UV/Vis Spectroscopic Titrations

Figure 8. Titration of 4 using aqueous fluoride extracted from toothpaste, followed by UV/vis spectroscopy.

δ 77.0 ppm). The NMR spectra were measured in CD₃CN. The UV/vis spectra were measured with a GENESYS 10S spectrophotometer using a quartz cell of 1 cm³. CH₃CN employed for UV/vis experiments was of high-performance liquid chromatography-grade. All employed reagents were purchased from commercial sources. Reagents and solvents were of the highest quality available and used as received. Thin layer chromatography was performed on silica gel plates visualized with a UV lamp at 254 nm. Flash chromatography was performed on Aldrich silica gel (70–230 mesh).

Syntheses. *Pyrrolyl Perezone Synthesis (2, 3).* To a solution of 1 (0.1 g, 0.3 mmol) dissolved in dichloromethane (DCM, 2.5 mL) was added pyrrole (0.1 mL, 1.45 mmol). The mixture was stirred for 10 min, then SiO₂ (1.0 g) was added, and the solvent was removed under vacuum. The reaction was kept at room temperature for 16 h. The residue was purified by flash column chromatography (Hex–EtOAc 4:1).

(R)-2-Hydroxy-6-methyl-3-(6-methylhept-5-en-2-yl)-5-(1H-pyrrol-2-yl)cyclohexa-2,5-diene-1,4-dione 2. ¹H NMR (400 MHz, chloroform-*d*): δ 11.01 (s, 1H), 7.37 (s, 1H), 7.09

(s, 1H), 6.79 (s, 1H), 6.39 (s, 1H), 5.08 (m, 1H), 3.17–2.97 (m, 1H), 2.31 (s, 4H), 2.03–1.72 (m, 4H), 1.68–1.39 (m, 6H), 1.32–1.09 (m, 3H). ¹³C NMR (100 MHz, chloroform-*d*): δ 190.84, 183.19, 150.99, 133.45, 131.42, 128.97, 126.42, 124.55, 123.89, 123.11, 119.18, 110.51, 34.18, 29.60, 26.74, 25.65, 18.35, 17.61, 14.40. mp 73–75 °C. LRMS (ESI) *m/z*: 314.17 [M + 1]. HRMS: 314.1756 [M + 1] (314.175619 estimated), yield 0.09 g, 68%.

(R)-2-Hydroxy-6-methyl-3-(6-methyl-5-oxoheptan-2-yl)-5-(1H-pyrrol-2-yl)cyclohexa-2,5-diene-1,4-dione 3. ¹H NMR (400 MHz, chloroform-*d*): δ 11.00 (s, 1H), 7.45 (s, 1H), 7.12 (td, *J* = 2.8, 1.2 Hz, 1H), 6.80 (ddd, *J* = 4.0, 2.4, 1.3 Hz, 1H), 6.39 (dtd, *J* = 3.9, 2.6, 0.5 Hz, 1H), 3.05 (ddt, *J* = 13.2, 9.3, 7.0 Hz, 1H), 2.55 (dq, *J* = 13.9, 6.9 Hz, 1H), 2.44–2.34 (m, 2H), 2.31 (s, 4H), 2.10–1.97 (m, 1H), 1.88 (ddt, *J* = 13.6, 9.1, 6.3 Hz, 1H), 1.25 (dd, *J* = 7.1, 0.5 Hz, 5H), 1.05 (ddd, *J* = 6.9, 2.7, 0.5 Hz, 8H). ¹³C NMR (100 MHz, chloroform-*d*): δ 214.61, 190.76, 182.99, 151.22, 133.48, 128.99, 126.35, 124.12, 122.10, 119.37, 110.62, 40.73, 38.93, 29.42, 28.00, 18.34, 18.31, 18.26, 14.45. LRMS(EI) *m/z* (rel. int.): 331 ([M + 2], 12), 330 ([M + 1], 35), 329 ([M+], 100), 311 (15), 244 (58), 230 (47). HRMS (FAB+): 330.1708 (estimated, 330.1705) yield 0.06 g, 44%, corresponding to the literature.³⁷

(R)-6,6'-(5,5'-(Propane-2,2-diyl)bis(1H-pyrrole-5,2-diyl))-bis(3-hydroxy-5-methyl-2-((R)-6-methyl-5-oxoheptan-2-yl)-cyclohexa-2,5-diene-1,4-dione) 4. In a round-bottom flask was added a solution of pyrrolyl perezone 3 (44 mg, 0.14 mmol) and acetone (1 mL). The solution was diluted with water (5 mL) and, while stirring, HCl 35% (10 μ L) was added to the formed mixture. The reaction mixture was stirred for 36 h at room temperature. The crude was neutralized with aqueous NaHCO₃ and extracted with DCM (3 \times 5 mL). The organic layer was dried over anhydrous Na₂SO₄, filtrated, and concentrated under reduced pressure. The crude was purified via flash column chromatography (Hex–AcOEt, 7:3) to give product 4 as a blue-violet solid; yield 25 mg, 53%, mp 150–152 °C. ¹H NMR (400 MHz, chloroform-*d*): δ 10.94 (s, 2H), 6.78 (s, 2H), 6.26 (s, 2H), 5.60 (s, 2H), 3.02 (m, 2H), 2.55 (m, 2H), 2.45–2.32 (m, 4H), 2.27 (s, 6H), 1.80–1.63 (m, 10H), 1.24 (s, 6H), 1.02 (d, *J* = 12.9 Hz, 12H). ¹³C NMR

(100 MHz, chloroform-*d*): δ 215.95, 192.13, 183.71, 152.38, 146.10, 133.89, 128.80, 126.82, 122.60, 121.30, 108.30, 77.79, 77.47, 77.15, 40.93, 39.17, 36.20, 29.84, 29.42, 28.58, 28.06, 18.36, 18.35, 14.54. HRMS (FAB+): [M + 1] 699.3577 (estimated: 699.3567).

NMR Studies on Host and Guest. The NMR experiments were performed in CD₃CN. To a 0.01 M solution of **4** in a deuterated solvent were added different equivalents of TBAF (1×10^{-2} M) until saturation and spectra were recorded.

UV/Vis Studies on Host and Guest. The UV/vis experiments were performed in CH₃CN (HPLC-grade). To a solution of 5×10^{-4} M of **4** were added different equivalents of TBAF (1×10^{-2} M) until saturation. To another solution of **4** at the same concentration were added different equivalents of Ni (ClO₄)₂ (1×10^{-2} M) until saturation. To a solution of 5×10^{-4} M of **4** previously saturated with Ni (ClO₄)₂ were added different equivalents of TBAF. To a solution of 5×10^{-4} M of **4** previously saturated with TBAF were added different equivalents of Ni (ClO₄)₂. The same protocol was applied to evaluate compounds **1–3**.

Method of Continuous Variations for Job's Plot. The UV/vis experiments were performed in CH₃CN (HPLC-grade). Solutions of compounds **2–4** (hosts) and TBAF (guest) were prepared at the same concentration (5×10^{-4} M). Solutions of host/guest (1 mL) were prepared for measurements as 100–0, 90–10, 80–20, 70–30, 60–40, 50–50, 40–60, 30–70, 20–80, 10–90, and 0–100 proportions..

■ ASSOCIATED CONTENT

Supporting Information

The Supporting Information is available free of charge at <https://pubs.acs.org/doi/10.1021/acsomega.1c01420>.

NMR spectra, UV/vis spectra, and stoichiometry of complexes between compounds and ionic species (PDF)

■ AUTHOR INFORMATION

Corresponding Author

Luis Chacón-García – Laboratorio de Diseño Molecular, Instituto de Investigaciones Químico-Biológicas, Morelia, Michoacán 58030, Mexico; orcid.org/0000-0001-8877-4817; Email: lchacon@umich.mx

Authors

Mario Valle-Sánchez – Laboratorio de Diseño Molecular, Instituto de Investigaciones Químico-Biológicas, Morelia, Michoacán 58030, Mexico

Claudia A. Contreras-Celedón – Laboratorio de Diseño Molecular, Instituto de Investigaciones Químico-Biológicas, Morelia, Michoacán 58030, Mexico

Adrián Ochoa-Terán – Centro de Graduados e Investigación en Química, Tecnológico Nacional de México/Instituto Tecnológico de Tijuana, 22510 Tijuana, Baja California, Mexico

Complete contact information is available at:

<https://pubs.acs.org/doi/10.1021/acsomega.1c01420>

Author Contributions

Conceptualization, M.V.-S. and L.C.-G.; methodology, investigation, and writing original draft, M.V.-S., A.O.-T., and L.C.-G.; visualization, M.V.-S.; and supervision and funding acquisition, C.A.C.-C. and L.C.-G.

Notes

The authors declare no competing financial interest.

■ ACKNOWLEDGMENTS

M.V.-S. acknowledges the financial support of CONACYT through a graduate scholarship (S93548/449658). The authors thank the support of CIC-UMSNH (CIC-UMSNH, grant no. 2.19) and Professor J. Betzabe González-Campos who kindly facilitated the access to the UV/vis equipment to carry out a part of this work.

■ REFERENCES

- (1) Smith, B. D. Smart Molecules for Imaging, Sensing and Health (SMITH). *Beilstein J. Org. Chem.* **2015**, *11*, 2540–2548.
- (2) Kohnke, F. H. Calixpyrroles: from Anion Ligands to Potential Anticancer Drugs. *Eur. J. Org. Chem.* **2020**, *2020*, 4261–4272.
- (3) Erbas-Cakmak, S.; Leigh, D. A.; McTernan, C. T.; Nussbaumer, A. L. Artificial Molecular Machines. *Chem. Rev.* **2015**, *115*, 10081–10206.
- (4) You, L.; Zha, D.; Anslyn, E. V. Recent Advances in Supramolecular Analytical Chemistry Using Optical Sensing. *Chem. Rev.* **2015**, *115*, 7840–7892.
- (5) Busschaert, N.; Caltagirone, C.; Van Rossom, W.; Gale, P. A. Applications of Supramolecular Anion Recognition. *Chem. Rev.* **2015**, *115*, 8038–8155.
- (6) Gale, P. A.; Caltagirone, C. Fluorescent and Colorimetric Sensors for Anionic Species. *Coord. Chem. Rev.* **2018**, *354*, 2–27.
- (7) Park, S.-H.; Park, S.-H.; Howe, E. N. W.; Hyun, J. Y.; Chen, L.-J.; Hwang, I.; Vargas-Zuñiga, G.; Busschaert, N.; Gale, P. A.; Sessler, J. L.; Shin, I. Determinants of Ion-Transporter Cancer Cell Death. *Chem* **2019**, *5*, 2079–2098.
- (8) Jomova, K.; Valko, M. Advances in Metal-Induced Oxidative Stress and Human Disease. *Toxicology* **2011**, *283*, 65–87.
- (9) NTP (National Toxicology Program). *Report on Carcinogens*, 14th ed.; U.S. Department of Health and Human Services, Public Health Service.: Research Triangle Park, NC, 2016.
- (10) Moustakas, M. The Role of Metal Ions in Biology, Biochemistry and Medicine. *Materials* **2021**, *14*, 549.
- (11) McConnell, A. J.; Beer, P. D. Heteroditopic Receptors for Ion-Pair Recognition. *Angew. Chem., Int. Ed.* **2012**, *51*, S052–S061.
- (12) Kim, S. K.; Sessler, J. L. Calix[4]Pyrrole-Based Ion Pair Receptors. *Acc. Chem. Res.* **2014**, *47*, 2525–2536.
- (13) Pearce, E. N.; Braverman, L. E. Environmental Pollutants and the Thyroid. *Best Pract. Res., Clin. Endocrinol. Metab.* **2009**, *23*, 801–813.
- (14) Grandjean, P.; Landrigan, P. J. Neurobehavioural Effects of Developmental Toxicity. *Lancet Neurol.* **2014**, *13*, 330–338.
- (15) Liu, W.; Oliver, A. G.; Smith, B. D. Stabilization and Extraction of Fluoride Anion Using a Tetralactam Receptor. *J. Org. Chem.* **2019**, *84*, 4050–4057.
- (16) Zhou, Y.; Zhang, J. F.; Yoon, J. Fluorescence and Colorimetric Chemosensors for Fluoride-Ion Detection. *Chem. Rev.* **2014**, *114*, 5511–5571.
- (17) Smith, B. D. Ion-Pair Recognition by Ditopic Macrocyclic Receptors. *Macrocyclic Chemistry: Current Trends and Future Perspectives*; Springer, 2005; pp 137–151.
- (18) Casnati, A.; Massera, C.; Pelizzi, N.; Stibor, I.; Pinkassik, E.; Ugozzoli, F.; Ungaro, R. A Novel Self-Assembled Supramolecular Architecture Involving Cation, Anion and a Calix[4]Arene Heteroditopic Receptor. *Tetrahedron Lett.* **2002**, *43*, 7311–7314.
- (19) Peng, S.; He, Q.; Vargas-Zuñiga, G. I.; Qin, L.; Hwang, I.; Kim, S. K.; Heo, N. J.; Lee, C.-H.; Dutta, R.; Sessler, J. L. Strapped Calix[4]Pyrroles: From Syntheses to Applications. *Chem. Soc. Rev.* **2020**, *49*, 865–907.
- (20) Lin, Z.-H.; Ou, S.-J.; Duan, C.-Y.; Zhang, B.-G.; Bai, Z.-P. Naked-Eye Detection of Fluoride Ion in Water: A Remarkably Selective Easy-to-Prepare Test Paper. *Chem. Commun.* **2006**, *2*, 624–626.

- (21) Vargas-Zúñiga, G. I.; Sessler, J. L. Pyrrole N–H Anion Complexes. *Coord. Chem. Rev.* **2017**, *345*, 281–296.
- (22) Lankshear, M. D.; Cowley, A. R.; Beer, P. D. Cooperative AND Receptor for Ion-Pairs. *Chem. Commun.* **2006**, *117*, 612–614.
- (23) Hong, C. M.; Bergman, R. G.; Raymond, K. N.; Toste, F. D. Self-Assembled Tetrahedral Hosts as Supramolecular Catalysts. *Acc. Chem. Res.* **2018**, *51*, 2447–2455.
- (24) Picci, G.; Bazzicalupi, C.; Coles, S. J.; Gratteri, P.; Isaia, F.; Lippolis, V.; Montis, R.; Murgia, S.; Nocentini, A.; Orton, J. B.; Caltagirone, C. Halogenated Isophthalamides and Dipicolineamides: The Role of the Halogen Substituents in the Anion Binding Properties. *Dalton Trans.* **2020**, *49*, 9231–9238.
- (25) Howe, E. N. W.; Bhadbhade, M.; Thordarson, P. Cooperativity and Complexity in the Binding of Anions and Cations to a Tetratopic Ion-Pair Host. *J. Am. Chem. Soc.* **2014**, *136*, 7505–7516.
- (26) Balraj, C.; Satheskumar, A.; Ganesh, K.; Elango, K. P. Charge Transfer Complexes of Quinones in Aqueous Medium: Spectroscopic and Theoretical Studies on Interaction of Cimetidine with Novel Substituted 1,4-Benzoquinones and Its Application in Colorimetric Sensing of Anions. *Spectrochim. Acta, Part A* **2013**, *114*, 256–266.
- (27) Jali, B. R.; Barick, A. K.; Mohapatra, P.; Sahoo, S. K. A Comprehensive Review on Quinones Based Fluoride Selective Colorimetric and Fluorescence Chemosensors. *J. Fluorine Chem.* **2021**, *244*, 109744.
- (28) Fan, D.; Zhang, B.; Deng, K. Colorimetric Sensing of Fluoride Based on Acenaphthenequinone 2, 4-Dinitrophenylhydrazone. *J. Mater. Sci. Eng. A* **2012**, *2*, 712–716.
- (29) McNaughton, D. A.; Fu, X.; Lewis, W.; D'Alessandro, D. M.; Gale, P. A. Hydroquinone-Based Anion Receptors for Redox-Switchable Chloride Binding. *Chemistry* **2019**, *1*, 80–88.
- (30) Kubota, Y.; Niwa, T.; Jin, J.; Funabiki, K.; Matsui, M. Synthesis, Absorption, and Electrochemical Properties of Quinoid-Type Bisboron Complexes with Highly Symmetrical Structures. *Org. Lett.* **2015**, *17*, 3174–3177.
- (31) Lankshear, M. D.; Dudley, I. M.; Chan, K.-M.; Cowley, A. R.; Santos, S. M.; Felix, V.; Beer, P. D. Cooperative and Ion-Pair Recognition by Heteroditopic Calix[4]Diquinone Receptors. *Chem.—Eur. J.* **2008**, *14*, 2248–2263.
- (32) Liu, K.; He, L.; He, X.; Guo, Y.; Shao, S.; Jiang, S. Calix[4]Pyrrole-TCBQ Assembly: A Signal Magnifier of TCBQ for Colorimetric Determining Amino Acids and Amines. *Tetrahedron Lett.* **2007**, *48*, 4275–4279.
- (33) Tapia-Juárez, M.; González-Campos, J. B.; Contreras-Celedón, C.; Corona, D.; Cuevas-Yañez, E.; Chacón-García, L. A New Type of Anion Receptor: Pyrrolyl Quinones. *RSC Adv.* **2014**, *4*, 5660.
- (34) Mejía-Farfán, I.; Solís-Hernández, M.; Navarro-Santos, P.; Contreras-Celedón, C. A.; Cortés-García, C. J.; Chacón-García, L. Oxidative Amidation of Benzaldehyde Using a Quinone/DMSO System as the Oxidizing Agent. *RSC Adv.* **2019**, *9*, 18265–18270.
- (35) Burgueño-Tapia, E.; González-Coloma, A.; Castillo, L.; Joseph-Nathan, P. Antifeedant and Phytotoxic Activity of Hydroxyperezone and Related Molecules. *Z. Naturforsch., C: J. Biosci.* **2008**, *63*, 221–225.
- (36) De La Peña, A.; Izaguirre, R.; Baños, G.; Viveros, M.; Enriquez, R. G.; Fernandez, J. M. Effect of Perezone, Aminoperezone and upon in Vitro Platelet Aggregation. *Phytomedicine* **2001**, *8*, 465–468.
- (37) Concepción Lozada, M.; Soria-Arteche, O.; Teresa Ramírez Apan, M.; Nieto-Camacho, A.; Enríquez, R. G.; Izquierdo, T.; Jiménez-Corona, A. Synthesis, Cytotoxic and Antioxidant Evaluations of Amino Derivatives from Perezone. *Bioorg. Med. Chem.* **2012**, *20*, 5077–5084.
- (38) Sánchez-Torres, L. E.; Torres-Martínez, J. A.; Godínez-Victoria, M.; Omar, J. M.; Velasco-Bejarano, B. Perezone and Its Isomer Isoperezone Induce Caspase-Dependent and Caspase-Independent Cell Death. *Phytomedicine* **2010**, *17*, 614–620.
- (39) Saha, I.; Lee, J. T.; Lee, C.-H. Recent Advancements in Calix[4]Pyrrole-Based Anion-Receptor Chemistry. *Eur. J. Org. Chem.* **2015**, *2015*, 3859–3885.
- (40) Chacón-García, L.; Valle-Sánchez, M.; Contreras-Celedón, C. A Novel Semisynthetic Anion Receptor: Synthesis and Ion Recognition of (1-H-Pyrrol-2-Yl)-4-Oxo-Perezone. *Lett. Org. Chem.* **2013**, *10*, 632–636.
- (41) Sobral, A. J. F. N.; Rebanda, N. G. C. L.; Da Silva, M.; Lampreia, S. H.; Ramos Silva, M.; Beja, A. M.; Paixão, J. A.; Rocha Gonsalves, A. M. D. One-Step Synthesis of Dipyrromethanes in Water. *Tetrahedron Lett.* **2003**, *44*, 3971–3973.
- (42) Littler, B. J.; Miller, M. A.; Hung, C.-H.; Wagner, R. W.; O'Shea, D. F.; Boyle, P. D.; Lindsey, J. S. Refined Synthesis of 5-Substituted Dipyrromethanes. *J. Org. Chem.* **1999**, *64*, 1391–1396.
- (43) Mejía-Farfán, I.; Contreras-Celedón, C.; Avina-Verduzco, J.; Chacon-Garcia, L. An Efficient Synthesis of Calix[4]Pyrroles Under Lewis Acid Conditions. *Lett. Org. Chem.* **2008**, *5*, 237–239.
- (44) Gómez-Serrano, G.; Cristiani-Urbina, E.; Villegas-Garrido, T. Time-Dependent Perezone Production in Different Culture Systems of *Acourtia Cordata*. *Cent. Eur. J. Biol.* **2012**, *7*, 507–518.
- (45) Thomson, R. H. Chapter 3—Benzoquinones. *Naturally Occurring Quinones*; Academic Press Inc.: New York, 1971, pp 125–130.
- (46) Mure, M.; Klinman, J. P. Model Studies of Topaquinone-Dependent Amine Oxidases. 1. Oxidation of Benzylamine by Topaquinone Analogs. *J. Am. Chem. Soc.* **1995**, *117*, 8698–8706.
- (47) Escobedo-González, R.; Vargas-Requena, C. L.; Moyers-Montoya, E.; Aceves-Hernández, J. M.; Nicolás-Vázquez, M. I.; Miranda-Ruvalcaba, R. In Silico Study of the Pharmacologic Properties and Cytotoxicity Pathways in Cancer Cells of Various Indolylquinone Analogues of Perezone. *Molecules* **2017**, *22*, 1060.
- (48) Gallardo-Alfonzo, S.; Cortés-García, C. J.; Mejía-Farfán, I.; López, Y.; Mojica, M.; Contreras-Celedón, C.; Chacón-García, L. A Two-Step Synthesis of a Novel 7,8-Dihydro-5,8-Ethanoindolizine-6,9(5H)-Dione. *Synlett* **2021**, *32*, 185–191.
- (49) Scheerder, J.; Engbersen, J. F. J.; Casnati, A.; Ungaro, R.; Reinhoudt, D. N. Complexation of Halide Anions and Tricarboxylate Anions by Neutral Urea-Derivatized p-Tert-Butylcalix[6]Arenes. *J. Org. Chem.* **1995**, *60*, 6448–6454.
- (50) Katayev, E. A.; Boev, N. V.; Khrustalev, V. N.; Ustyniuk, Y. A.; Tananaev, I. G.; Sessler, J. L. Bipyrrole- and Dipyrromethane-Based Amido-Imine Hybrid Macrocycles. New Receptors for Oxoanions. *J. Org. Chem.* **2007**, *72*, 2886–2896.
- (51) Gupta, V. K.; Mergu, N.; Singh, A. K. Fluorescent Chemosensors for Zn²⁺ Ions Based on Flavonol Derivatives. *Sens. Actuators, B* **2014**, *202*, 674–682.
- (52) Mir, M. A.; Ashraf, M. W. Chelate Formation and Stability Analysis of Cobalt, Nickel and Copper with Lomatol. *Arabian J. Chem.* **2021**, *14*, 102930.
- (53) Escobedo-González, R. G.; Pérez Martínez, H.; Nicolás-Vázquez, M. I.; Martínez, J.; Gómez, G.; Serrano, J. N.; Carranza Téllez, V.; Vargas-Requena, C. L.; Miranda Ruvalcaba, R. Green Production of Indolylquinones, Derivatives of Perezone, and Related Molecules, Promising Antineoplastic Compounds. *J. Chem.* **2016**, *2016*, 3870529.
- (54) Lion, D. C.; Baudry, R.; Hedayatullah, M.; Da Conceição, L.; Genard, S.; Maignan, J. Reaction of 2,5-dimethylpyrroles with quinones. Synthesis of new pyrrolylquinones. *J. Heterocycl. Chem.* **2002**, *39*, 125–130.
- (55) Karlsson, C.; Huang, H.; Strømme, M.; Gogoll, A.; Sjödin, M. Ion- and Electron Transport in Pyrrole/Quinone Conducting Redox Polymers Investigated by in Situ Conductivity Methods. *Electrochim. Acta* **2015**, *179*, 336–342.